

Oil & Natural Gas Technology

DOE Award No.: DE-FE0009897

Quarterly Research Performance Progress Report (Period ending 3/31/2016)

Hydrate-Bearing Clayey Sediments: Morphology, Physical Properties, Production and Engineering/Geological Implications

Project Period (10/1/2012 to 9/30/2016)

Submitted by:
J. Carlos Santamarina



Georgia Institute of Technology
DUNS #: 097394084
505 10th street
Atlanta , GA 30332
e-mail: jcs@gatech.edu
Phone number: (404) 894-7605

Prepared for:
United States Department of Energy
National Energy Technology Laboratory

Submission date: 4/30/2016



Office of Fossil Energy

DISCLAIMER:

This report was prepared as an account of work sponsored by an agency of the United States Government. Neither the United States Government nor any agency thereof, nor any of their employees, makes any warranty, express or implied, or assumes any legal liability or responsibility for the accuracy, completeness, or usefulness of any information, apparatus, product, or process disclosed, or represents that its use would not infringe privately owned rights. Reference herein to any specific commercial product, process, or service by trade name, trademark, manufacturer, or otherwise does not necessarily constitute or imply its endorsement, recommendation, or favoring by the United States Government or any agency thereof. The views and opinions of authors expressed herein do not necessarily state or reflect those of the United States Government or any agency thereof.

ACCOMPLISHMENTS

Context – Goals. *Fine grained sediments host more than 90% of the global gas hydrate accumulations. Yet, hydrate formation in clayey sediments is least understood and characterized. This research focuses on hydrate bearing clayey sediments. The goals of this research are (1) to gain a fundamental understanding of hydrate formation and ensuing morphology, (2) to develop laboratory techniques to emulate “natural” formations, (3) to assess and develop analytical tools to predict physical properties, (4) to evaluate engineering and geological implications, and (5) to advance gas production alternatives to recover methane from these sediments.*

Accomplished

The main accomplishments for this period include:

- Gas migration in soft sediments – Emphasis on shallow marine accumulations
 - Experimental studies
- Critical pore size for nucleation
- Stress field analysis leading to different crystal morphologies
- Impact of heterogeneity on small strain stiffness

Plan - Next reporting period

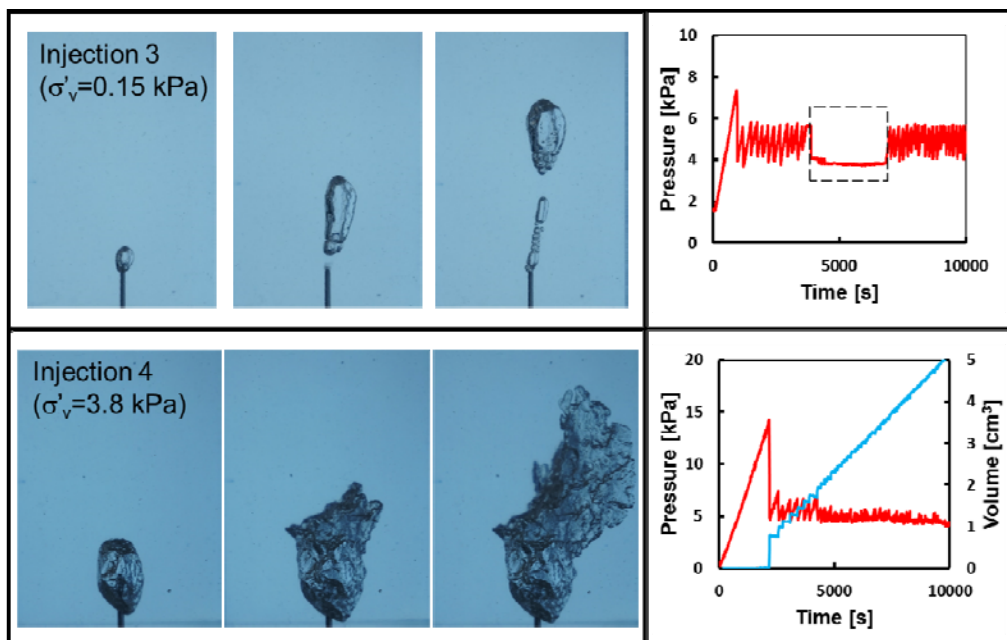
1. Advance understanding of crystal-sediment interaction.
2. Advance numerical experiments to predict properties.
3. Gas Migration in Soft Sediments
 - Theoretical Analysis
 - Numerical Simulation
4. Investigate P- and S-wave signatures in ice-bearing kaolinite clays (as analogue for hydrate bearing clay) at various stress conditions.
5. Visualize ice morphology in clays by 3D X-ray tomography.

RESEARCH IN PROGRESS

Gas Migration in Shallow Sediments

Gas injection tests were conducted at different effective stress conditions (from 0.15 kPa to 44 kPa) to simulate gas migration in the sea floor in view of potential hydrate accumulations at shallow depth. Figure 1 summarizes these results. Images recorded during the tests show the process of gas inclusion growth. The gas pressure (blue line) was measured using a pressure transducer, and the volume of the gas inclusion (red line) in the transparent soil was calculated based on the pressure-volume relationship (Ideal Gas Law).

Figure 2 shows the influence of the sediment stiffness on the evolving morphology of the gaseous body. Tubes and bubbles were observed at very low effective stress. A transition from cavity expansion to opening-mode “fractures” was observed at an effective stress around 4 kPa. At higher effective stress, gas migrated as a thin fracture. The calculated thickness to width ratio for the different gaseous bodies decreases as the sediment stiffness increases.



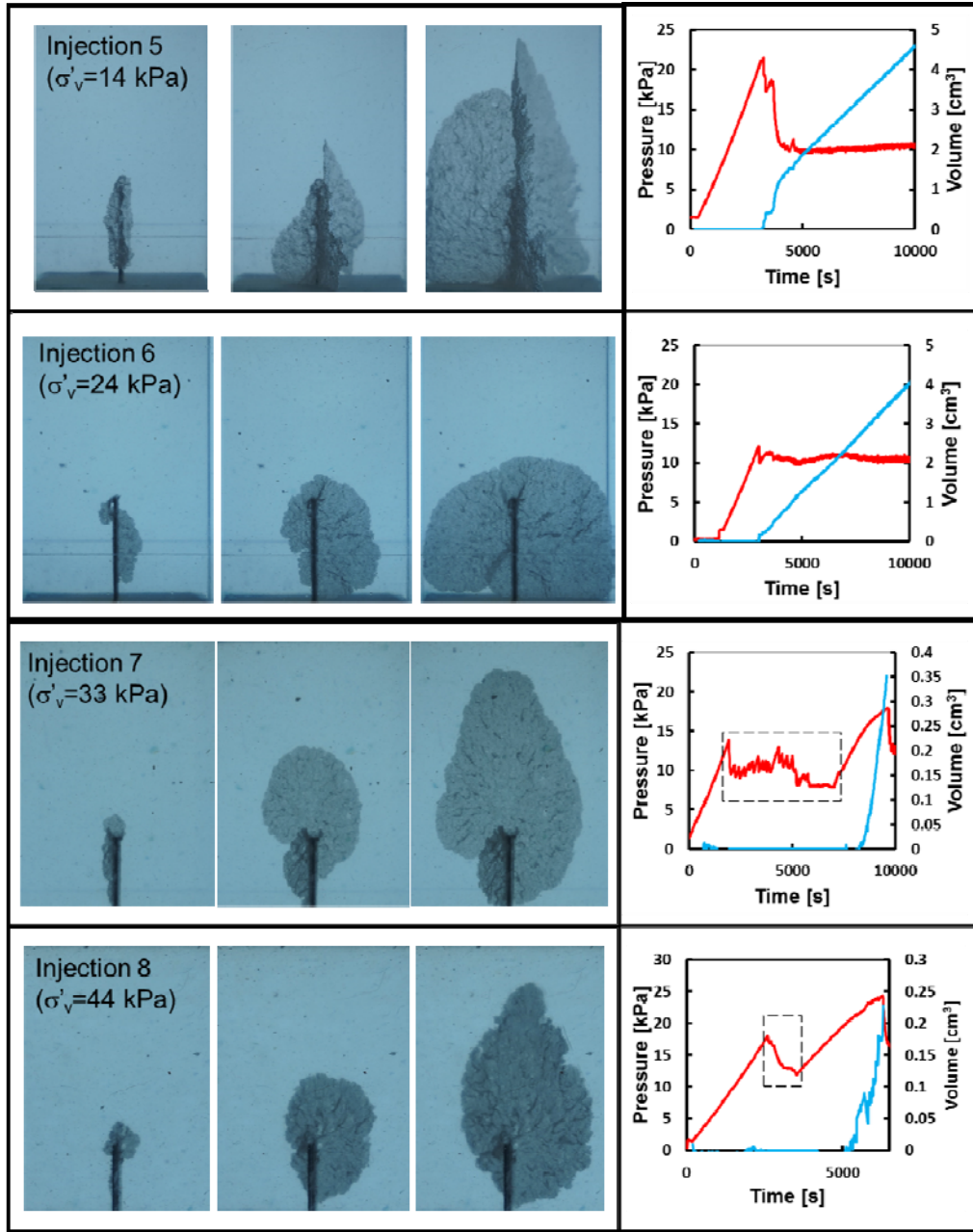


Figure 1. Summary of Injection Tests Results.

The relationship between gas injection pressure and vertical effective stress is shown in figure 3. It should be noted that injection started with an existing small discontinuity for tests with effective stress equal to 24, 33 and 44 kPa. Gas injection pressures for these conditions are very close to the estimated horizontal effective stress. Blue dots may relate to global cavity failure.

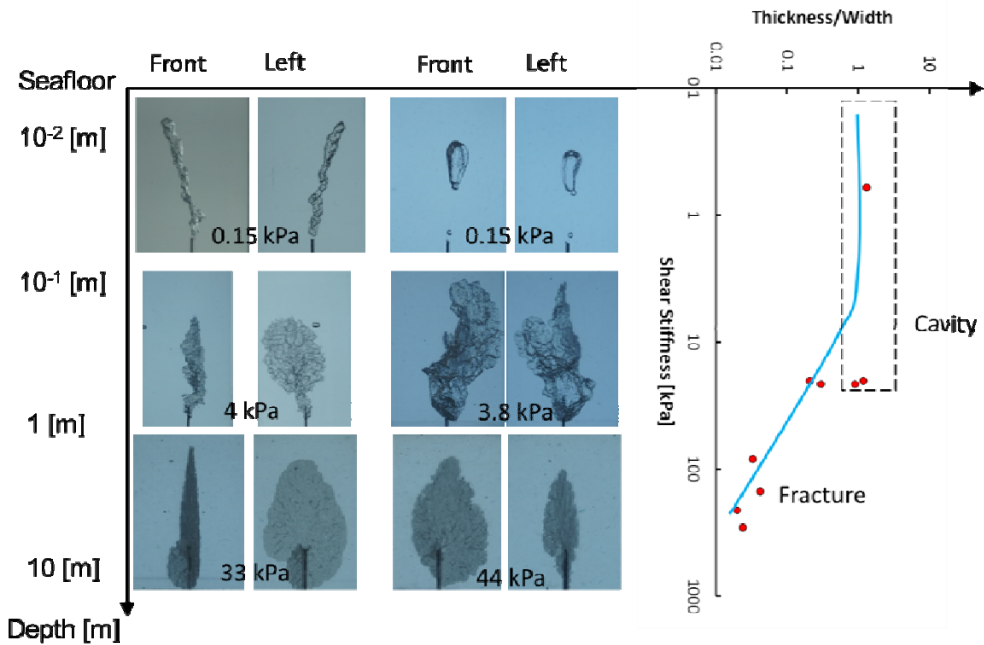


Figure 2. Gas Morphology in Soft Sediments.

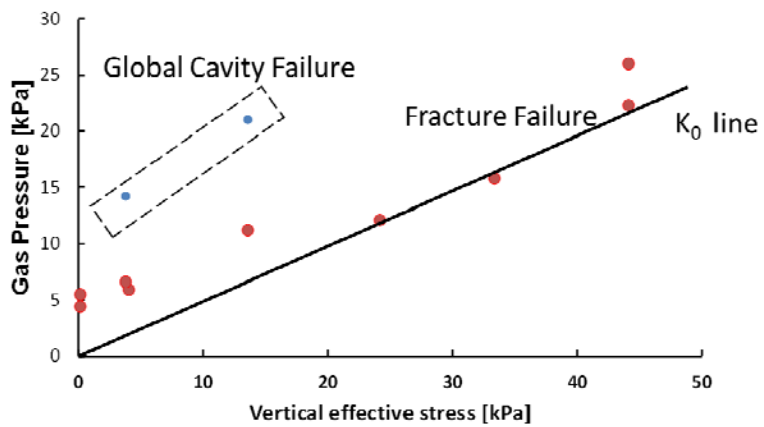


Figure 3. Gas Injection Pressure versus Vertical Effective Stress.

Cyclic Loading Results. The effect of cyclic loading was also examined to simulate tidal cycles. During unloading, gas expanded and advanced the cavity as it migrated upwards. During reloading, the cavity partially closed (figure 4). The long-term effects of cyclic loading remain unclear at this stage.

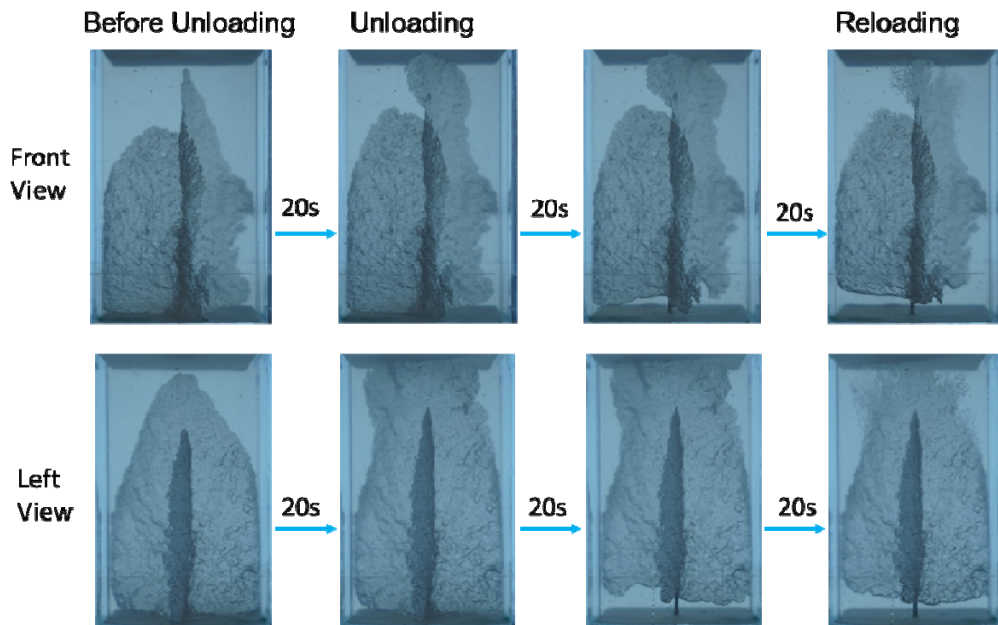


Figure 4. Unloading and Reloading Tests for sample at original effective stress of 14 kPa.

Memory Effect. Injection sequences exhibit clear memory effects. After first injection, the gas inclusion gradually closes, probably as a result of gas dissolution into the medium. During the second injection, gas invaded the sediment at a lower injection pressure and following the same pathway created by the first injection. Memory of the preferential pathway remains in the sediment even when additional gas injection is not attempted for long inactive periods.

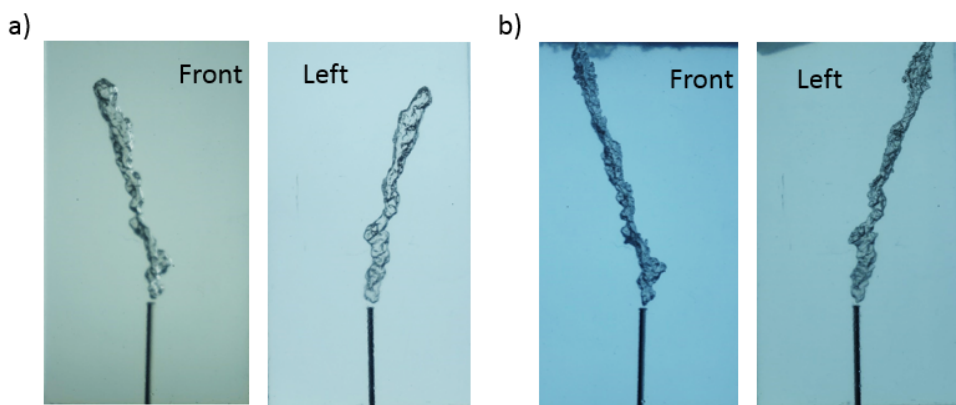


Figure 5. Comparison between gas morphology during the first injection (left images) and the second injection (21 hours after the first injection – images on the right). Case: low effective stress 0.15 kPa.

Critical pore size for nucleation

Let's consider the following initial conditions: an isolated pore of diameter d_p , critical nuclei size diameter d_c for a given pressure and temperature condition, solute concentration before nucleation c_s , and solute concentration c_0 after nucleation and in equilibrium with the crystal that formed. Under these conditions, the minimum pore size for nucleation to happen within a pore and without solute exchange with adjacent pores should satisfy the mass conservation of the solute:

$$c_s \frac{3\pi}{32} (d_p)^3 = \frac{3\pi}{32} (d_c)^3 + c_0 \frac{3\pi}{32} ((d_p)^3 - (d_c)^3)$$

$$d_p = d_c \left(\frac{1 - c_0}{c_s - c_0} \right)^{1/3}$$

where concentrations are specified in terms of volume of solute/volume of solution

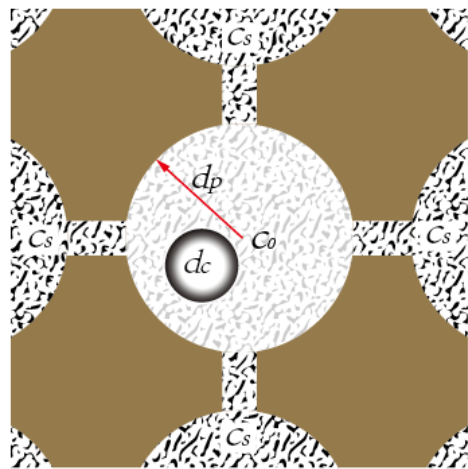


Figure 6: Nucleation in pores

Substances such as methane require large pores or high supersaturation to nucleate in pores as diffusive transport between pores may not be fast enough to sustain the growth of an incipient nucleation. Therefore, this analysis highlights that the probability of stable hydrate nuclei decreases in small pores.

Nodules or lenses: stress field analysis

Natural crystals exhibit different morphologies when nucleation and growth take place in different conditions. Figure 7 shows gypsum formations in sediments in the form of nodules, roses and roses with blades.



Figure 7: Gypsum crystal in different field conditions (left: <http://www.southampton.ac.uk>; center and right: <http://legacy.earlham.edu>)

Figure 8 shows the principle stress field. Crystal growth into the minimum principal stress and in the direction of the main principle stress is favored. In all cases, the crystal senses the local stress field.

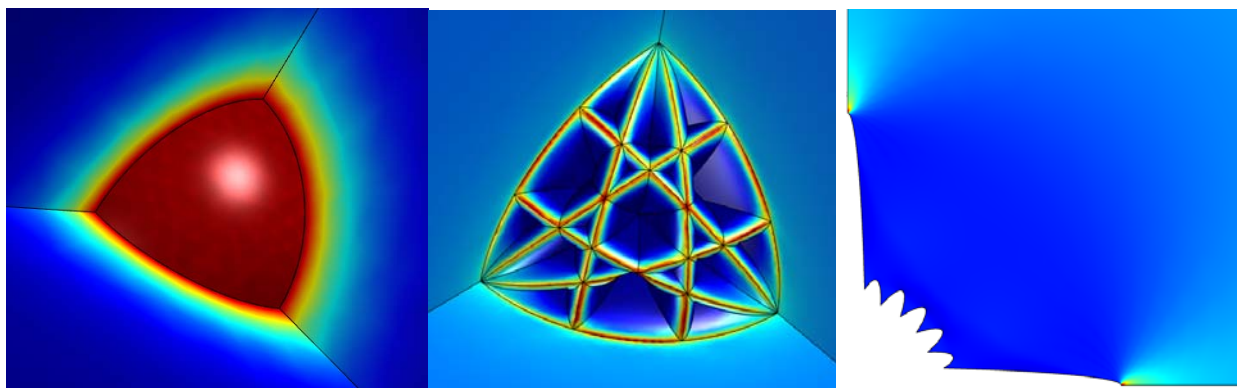


Figure 8: The minimum principle stress field.

Impacts of heterogeneity on small-strain stiffness

Hydrate in fine-grained sediments tends to manifest in pervasive lenses, which cause heterogeneity and anisotropy in all the physical properties of hydrate-bearing clayey sediments. We designed and built a high pressure aluminum effective-stress cell to measure P- and S-wave velocities at various load conditions with concurrent 3D X-ray imaging to capture the internal lens structure.

Preliminary results were obtained using frozen soil as an analogue of hydrate-bearing soils. Fine sands (F110, US silica) are mixed with a predetermined amount of water to achieve 30% ice saturation in sands upon freezing. Initial distributions of water in sands are intentionally controlled to generate different patterns. Specifically, the parallel model is made of water-saturated sand columns embedded in dry sands; the patchy model is a patchy of water-saturated sands embedded in the dry sand matrix (in this case the ice-bearing sand patch forms close to the receiver); the homogeneous model is generated by uniformly mixing sands with water within a plastic bag before being remolded in the test cell. The series model is created by water evaporation at the top of the specimen.

All wave signatures shown below are obtained when the specimens are subjected to 100kPa effective stress under zero-lateral strain condition and the temperature is -5°C. Measured P- and S-wave velocities vary for sands with the same amount ice saturation but different distribution morphologies. The dominant frequency in received wave signatures increases with the number of ice grains – Note: refer to the wave signatures in patchy and homogeneous cases. The ice distribution morphology in sands also results in evident differences in wave amplitude and attenuation (note y-axis are in different scales). In summary, wave velocity reflects specimen bulk stiffness; amplitude and characteristic frequency capture specimen heterogeneity and ice distribution morphologies.

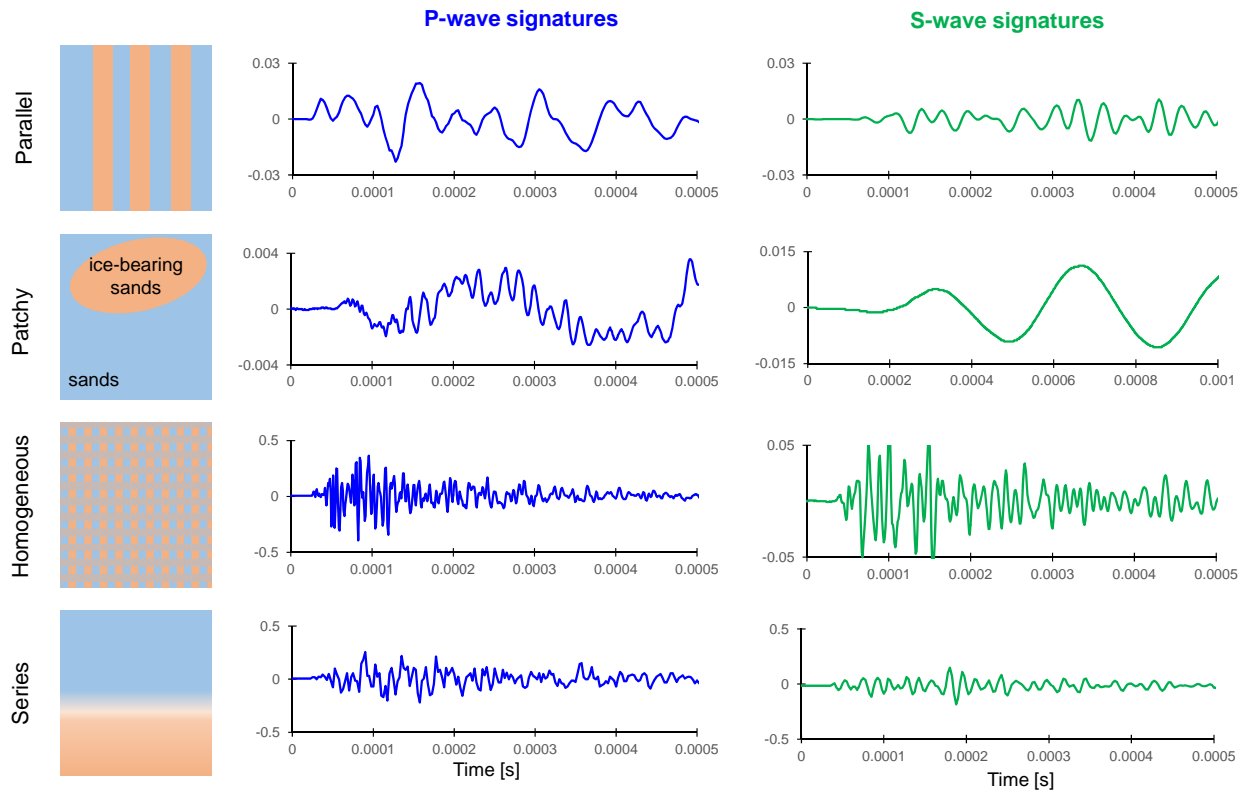


Figure 9. P- and S-wave signatures for ice-bearing sands: The effects of heterogeneity. Ice distribution affects wave velocities, amplitude (i.e., attenuation) and the characteristic frequency content of the signatures.

MILESTONE LOG

Milestone	Planned completion date	Actual completion date	Verification method	Comments
Literature review	5/2013	5/2013	Report	
Preliminary laboratory protocol	8/2013	8/2013	Report (with preliminary validation data)	
Cells for Micro-CT	8/2013	8/2013	Report (with first images)	
Compilation of CT images: segregated hydrate in clayey sediments	8/2014	8/2014	Report (with images)	
Preliminary experimental studies on gas production	12/2014	12/2014	Report (with images)	
Analytical/numerical study of 2-media physical properties	5/2015	5/2015	Report (with analytical and numerical data)	Additional studies in progress
Experimental studies on gas production	12/2015	12/2015	Report (with data)	Additional studies in progress
Early numerical results related to gas production	5/2016	In progress	Report	
Comprehensive results (includes Implications)	9/2016	In progress	Comprehensive Report	

PRODUCTS

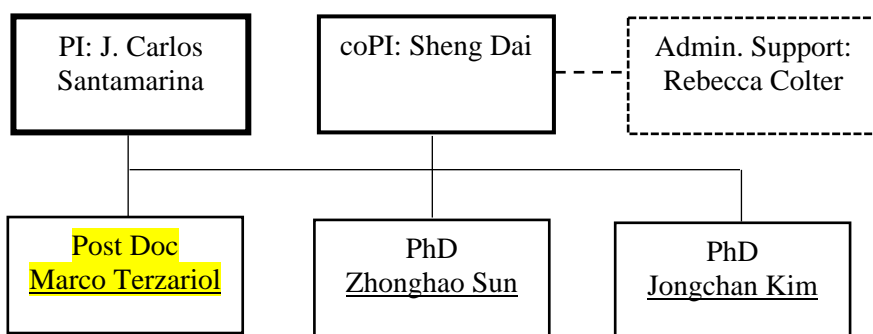
- **Publications & Presentations:**
In progress
- **Website:** Publications and key presentations are included in <http://pmrl.ce.gatech.edu/> (for academic purposes only)
- **Technologies or techniques:** X-ray tomographer and X-ray transparent pressure vessel
- **Inventions, patent applications, and/or licenses:** None at this point.
- **Other products:** None at this point.

PARTICIPANTS & OTHER COLLABORATING ORGANIZATIONS

Research Team: The current team involves:

- Liang Lei (PhD student)
- Zhonghao Sun (PhD student)
- Sheng Dai (Assistant Professor)
- Carlos Santamarina (Professor)

Research Team:



IMPACT

Understanding of fine grained hydrate-bearing sediments.

CHANGES/PROBLEMS:

None at this point.

SPECIAL REPORTING REQUIREMENTS:

We are progressing towards all goals for this project.

BUDGETARY INFORMATION:

As of the end of this research period, expenditures are summarized in the following table.

Note: in our academic cycle, higher expenditures typically take place during the summer quarter.

		Budget Period 4							
		Q1		Q2		Q3		Q4	
		10/1/15 - 12/31/15		1/1/16 - 3/31/16		4/1/16 - 6/30/16		7/1/16 - 9/30/16	
		Q1	Cumulative Total	Q2	Cumulative Total	Q3	Cumulative Total	Q4	Cumulative Total
Baseline Reporting Quarter									
	DE-FE009897								
Baseline Cost Plan									
Federal Share	41,547	502,751	41,547	544,299	41,547	585,846	41,547	627,393	
Non-Federal Share	11,935	146,969	11,935	158,904	11,935	170,839	11,935	182,774	
Total Planned	53,482	649,720	53,482	703,203	53,482	756,685	53,482	810,167	
Actual Incurred Cost									
Federal Share	22,802	461,960	32,381	494,341					
Non-Federal Share	15,167	152,445	10,111	162,556					
Total Incurred Costs	37,969	614,405	42,492	656,897					
Variance									
Federal Share	-18,745	-40,791	-9,166	-49,957					
Non-Federal Share	3,232	5,476	-1,824	3,652					
Total Variance	-15,513	-35,315	-10,990	-46,305					

National Energy Technology Laboratory

626 Cochran's Mill Road
P.O. Box 10940
Pittsburgh, PA 15236-0940

3610 Collins Ferry Road
P.O. Box 880
Morgantown, WV 26507-0880

13131 Dairy Ashford Road, Suite 225
Sugar Land, TX 77478

1450 Queen Avenue SW
Albany, OR 97321-2198

Arctic Energy Office
420 L Street, Suite 305
Anchorage, AK 99501

Visit the NETL website at:
www.netl.doe.gov

Customer Service Line:
1-800-553-7681

